HHS Public Access

Author manuscript

J Biophotonics. Author manuscript; available in PMC 2019 September 01.

Published in final edited form as:

J Biophotonics. 2018 September ; 11(9): e201700289. doi:10.1002/jbio.201700289.

Time-lapse microscopy of oxidative stress demonstrates metabolic sensitivity of retinal pericytes under high glucose condition

Zahra Ghanian[1], **Shima Mehrvar**[1], **Nasim Jamali**[2,3], **Nader Sheibani**[2,3,#], and **Mahsa Ranji**[1,#,*]

[1]Department of Electrical Engineering, University of Wisconsin-Milwaukee, Milwaukee, WI, US

[2]Departments of Ophthalmology and Visual Sciences, Biomedical Engineering, and Cell and Regenerative Biology, University of Wisconsin School of Medicine and Public Health, Madison, WI, US

[3]McPherson Eye Research Institute, University of Wisconsin School of Medicine and Public Health, Madison, WI, US

Abstract

Hyperglycemia affects retinal vascular cell function, promotes the development and progression of diabetic retinopathy, and ultimately causes vision loss. Oxidative stress, reactive oxygen species (ROS) in excess, is a key biomarker for diabetic retinopathy. Using time-lapse fluorescence microscopy, ROS dynamics was monitored and the metabolic resistivity of retinal endothelial cells (REC) and pericytes (RPC) was compared under metabolic stress conditions including high glucose (HG). In the presence of a mitochondrial stressor REC exhibited a significant increase in the rate of ROS production compared with RPC. Thus, under normal glucose (NG), REC may utilize oxidative metabolism as the bioenergetic source, while RPC metabolic activity is independent of mitochondrial respiration. In HG condition, the rate of ROS production in RPC was significantly higher, whereas this rate remained unchanged in REC. Thus, under HG condition RPC may preferentially utilize oxidative metabolism, which results in increased rate of ROS production. In contrast, REC use glycolysis as their major bioenergetic source for ATP production, and consequently HG minimally affect their ROS levels. These observations are consistent with our previous studies where we showed HG condition has minimal effect on apoptosis of REC, but results in increased rate of apoptosis in RPC. Collectively, our results suggest that REC and RPC exhibit different metabolic activity preferences under different glucose conditions. Thus, protection of RPC from oxidative stress may provide an early point of intervention in development and progression of diabetic retinopathy.

Keywords

time-lapse microscopy; diabetic retinopathy; high glucose; glycolysis; oxidative stress; mitochondrial stressor; Mito-SOX; retinal endothelial cell; retinal pericyte

* ranji@uwm.edu.
# Co-senior authors

1. Introduction

Increased oxidative stress and mitochondrial dysfunction have been linked to the development and progression of diabetic retinopathy, and trigger the pro-apoptotic actions of mitochondria [1, 2]. Specifically, oxidative stress plays a key role in retinal vascular cell injury and degeneration of capillaries during diabetes [2]. However, little is known about the primary retinal vascular cell target and the mechanism(s) involved in metabolic stress associated with diabetes and pathogenesis of diabetic retinopathy.

The distribution of vascular pericytes (PC) and endothelial cells (EC) reflect specific functional features of the microvasculature in different organs and relate to the organ metabolic demand and specialized cellular functions. The greatest PC density has been noted in the retinal blood vessels, which is needed for the particularly high metabolic activity of the retina, and requires meticulously regulated blood flow. The greater pericyte number and coverage has been linked to higher capillary and venular blood flow and better microvascular barrier. Due to the important role of retinal pericytes (RPC) in controlling blood flow, a higher sensitivity to metabolic changes is expected for these cells compared with retinal endothelial cells (REC), especially under stress conditions. We previously showed that RPC are more sensitive to adverse effects of high glucose compared with REC [3, 4]. However, the reason for this selective sensitivity remains unknown. We proposed this sensitivity may be linked to preferences of bioenergetic sources for these cells.

Here, we measured the metabolic resistivity of the RPC and REC by monitoring reactive oxygen species (ROS) production in real-time, while the live cells were challenged with various metabolic stressors. Stress conditions were induced by a mitochondrial uncoupler or inhibitors of electron transport chain (ETC) complexes affecting the oxidative metabolic pathway. Moreover, the metabolic stress was exacerbated by HG condition to gain insight into the underlying cause of RPC sensitivity to HG. Using time-lapse microscopy, an experimental protocol was previously designed to quantify dynamics of ROS production in vitro [5, 6]. In this protocol, nano-molar concentration of MitoSOX red was used to monitor mitochondrial ROS production level and the rate in live cells over time. Using this experimental protocol, the dynamics of ROS production in REC and RPC were determined. Live cells were incubated with PCP (a mitochondrial uncoupler) or rotenone and antimycin A (mitochondrial ETC inhibitors) under normal glucose (NG). Furthermore, the mitochondrial stress from PCP treatment was compared under HG.

2. Materials and Methods

2.1. Cell preparation

RPC and REC were isolated from C57BL/6J Immorto mice as previously described [7, 8]. Briefly, eyes were enucleated and hemisected. The retinas were dissected out aseptically under a dissecting microscope and kept in serum-free DMEM containing penicillin/streptomycin (Sigma, St. Louis, MO). Retinas (12 to 14 from one litter) were pooled together, rinsed with serum-free DMEM, minced into small pieces in a 60-mm tissue culture dish using sterilized razor blades, and digested in 5 ml of collagenase type I (1 mg/ml in

serum-free DMEM, Worthington, Lakewood, NJ) for 30–45 min at 37°C. Following digestion, DMEM with 10% FBS was added and cells were pelleted. The cellular digests were then filtered through a double layer of sterile 40 μm nylon mesh (Sefar America Inc., Fisher Scientific, Hanover Park, IL), centrifuged at 400 xg for 10 min to pellet cells, and cells were washed twice with DMEM containing 10% FBS. The cells were resuspended in 1.5 ml medium (low glucose DMEM; 5 mM with 10% FBS) and incubated with sheep anti-rat magnetic beads pre-coated with anti-PECAM-1. After affinity binding, magnetic beads were washed six times with DMEM with 10% FBS and bound cells in EC growth medium were plated into a single well of a 24 well plate pre-coated with 2 μg/ml of human fibronectin (BD Biosciences, Bedford, MA). Endothelial cells were grown in DMEM containing 10% FBS, 2 mM L-glutamine, 2 mM sodium pyruvate, 20 mM HEPES, 1% non-essential amino acids, 100 μg/ml streptomycin, 100 U/ml penicillin, freshly added heparin at 55 U/ml (Sigma, St. Louis, MO), endothelial growth supplement 100 μg/ml (Sigma, St. Louis, MO), and murine recombinant interferon-γ (R & D, Minneapolis, MN) at 44 units/ml. Cells were maintained at 33°C with 5% CO2. REC were progressively passed to larger plates, maintained, and propagated in 1% gelatin-coated 60 mm dishes (Falcon-BD Labware, Bedford, MA) [7, 8]. For isolation of RPC, the dissociated retinal cells, prepared above, were directly plated on uncoated wells of a 24 well plate, and progressively expanded in uncoated 60-mm tissue culture plates and maintained as previously described [9]. The RPC were maintained in DMEM containing 10% FBS, 2 mM L-glutamine, and murine recombinant interferon-γ (R & D) at 44 units/ml.

For imaging, REC were passed and cultured on gelatin-coated, while RPC were cultured on uncoated, 8-well chamber slide (4×104 cells/well, LabTekII, ThermoFisher) and incubated in low glucose (normal glucose; NG) growth medium for 24 hours. To determine the effect of HG on cellular metabolic resistivity and ROS production, cells were grown in medium with different glucose concentrations. Following 24 hours of incubation, cells were fed in 2–3 wells with high glucose (HG, 30 mM) medium, 2–3 wells with normal glucose (NG, 5 mM) medium, and 2–3 wells with D-glucose (5 mM) plus L-glucose (25 mM) for osmolarity control (OS) for 3 days. Following exposure to various glucose conditions, live cells were imaged using fluorescence microscopy. Before imaging, cells were subjected to nuclei staining, and during the imaging, the intracellular ROS level was determined by a mitochondrial-targeted red fluorescence probe, MitoSOX. All experiments were performed with cells between passages 9 to 11.

2.2. Fluorescent Probes

To measure the mitochondrial ROS production rate, and hence the metabolic resistivity of REC and RPC, cells were stained with 400 nM MitoSOX (Invitrogen M36008; excitation/emission: 510/580 nm) during the experiment. MitoSOX was kept in the medium while imaging. In order to maintain focus during imaging, the cells nuclei were also stained before imaging with 200 nM Hoechst (Life Technologies H1399, excitation/emission: UV/blue) and incubated in medium containing Hoechst for 30 minutes. Following incubation, the cells were rinsed twice with Hank’s Balanced Salt Solution (HBSS, Life Technologies 14025092). After washing, HBSS was added for subsequent fluorescent imaging. Hoechst

stains nuclei, whereas MitoSOX stains mitochondria ROS upon oxidation under appropriate excitation wavelength.

2.3. Fluorescence Microscopy

Cells were imaged live using a fluorescence microscope (Nikon Ti-E inverted) with a 20X objective and a scale of 0.32 μm per pixel. The cells were kept at 33±0.5°C in a 5% CO2 humidified chamber (Okolab) housed around the microscope, providing gas exchange and controlled temperature for time-lapse imaging over several hours. During the experiments, the level of O2 and CO2 inside the chamber was continuously monitored with an O2-BTA model O2 sensor and CO2-BTA model CO2 probe (Vernier Co., Beaverton, OR). Time-lapse images were obtained in the blue (Hoechst), and red (MitoSOX) channels to monitor nuclei, and mitochondrial ROS levels (Fig. 1). Eight fields of view (FOV) of cells were imaged including one FOV in each chamber of the bottom-glass plate. Stained cells with Hoechst and MitoSOX were subjected to 340–380 nm and 528–553 nm excitation source, and emission was recorded through 435–485nm and 590–650nm band-pass filters [5]. The images were captured using a charge-coupled device camera (Q-imaging, Aqua Exi, 14-bit, 6.45μm per pixel) with the exposure time of 0.68 μsec/pixel in the red channel. Fields that were imaged were selected on random by randomly moving the x- and y-axis drivers on the microscope stage. The fields that had a representative number of cells were then imaged.

Our experimental protocol [6, 10, 11] was designed to measure changes in mitochondrial ROS production associated with metabolic stress conditions as a model of ROS mediated injuries. Time-lapse images of FOV were captured in blue, and red channels, all in 70-sec intervals for 80 min. Ten min of baseline imaging was followed by the addition of MitoSOX (400 nM) to the live cells. Imaging was continued for 20 min after the addition of MitoSOX. Cells were then treated with pentachlorophenol sodium salt (PCP, chain uncoupler, 5 μM, Sigma Aldrich; 76480), rotenone (Complex I inhibitor, 25 μM, Sigma Aldrich; R8875), antimycin A (Complex III inhibitor, 10 μM, Sigma Aldrich; A8674) to study ROS production in the mitochondria as indicated by fluorescence intensity. Image acquisition continued for 50 min after adding the metabolic stressors.

2.4. Data analysis

The cell contours were detected in the bright field images using our cell segmentation algorithm [11]. The obtained mask including the cell contours was then applied to the time-lapse image stack in the red fluorescent channel. The nuclei were also identified in the blue images and the resulting blue binary image was used as a mask for the stack of the red images to exclude the nuclei contribution to the red intensity profiles. The mean intensity of the mitochondria in red channel image stack was calculated as a raw intensity profile over time.

Our developed methodology to obtain final intensity profiles of the cells from the input fluorescent images was previously reported [6]. The intensity profile of the red fluorescence images shows the dynamic of ROS production in response to MitoSOX (t=10 min) and metabolic stressors (t=30 min). In order to quantify the ROS levels and compare the changes in ROS production rate between RPC and REC, the raw intensity profiles were first

background subtracted. Day-to-day variation of light intensity and illumination pattern led to variations in the basal level intensity, which was accounted for background subtraction. Then the slope of the linear fit of the intensity profiles was calculated in either the MitoSOX interval (t=11–29 min) for the control group (with only MitoSOX treatment) or stress interval (t=30–35 min) for the treated group with stressors, respectively. The slope of the intensity profile in stress interval reflects ROS initiation rate.

2.5. Statistical analysis

Data are shown as means ± SE. Student's t-test was used for normally distributed data. A p-value < 0.05 was considered significant.

3. Results

In microscopic images captured in fluorescent channels, the nuclei were targeted by Hoechst in blue, and mitochondrial compartments were detected by MitoSOX in red. Panels a and b in Fig. 1 show the overlay of the blue and red fluorescent markers in REC and RPC. Panels c and d in Fig. 1 demonstrate changes in the fluorescence intensity of the REC (red profiles) and RPC (blue profiles) over time under NG and HG. Panel c and d compare the metabolic resistivity of REC with RPC under NG and HG. Fig. 1(c) shows that the metabolic properties of REC and RPC were different even at normal glucose level. However, under high glucose condition (Fig. 1(d)), RPC produced more mitochondrial ROS while REC did not exceed the level reached in NG.

Fig. 2 shows the corresponding quantitative changes in the fluorescence intensity of the REC (red curves) and RPC (blue curves) over time. Uncoupling and inhibiting mitochondrial ETC complexes (top panel and two bottom panels, respectively) significantly increased the rate of ROS production in both cell types when compared to the baseline rate of ROS production. Fig. 2 also demonstrates that uncoupling of the REC mitochondria with PCP resulted in an abrupt and marked increase in the rate of ROS production when compared with inhibitors of ETC complexes. Enhanced fluorescence intensity was evident right after addition of the mitochondrial stressors, and the intensity increased continuously over time, demonstrating a time-dependent amplification of ROS production.

Fig. 2 demonstrates that incubation of cells with an oxidizing agent (PCP; 5 μM), or reducing agents (ROT; 25 μM, and AA; 10 μM) resulted in significantly larger increase in the initial rate of ROS production (PCP: 8.27 ±0.97, 1.58 ± 0.47; ROT: 3.13 ± 0.24, 1.03 ± 0.18; AA: 10.74 ± 0.86, 1.96 ± 0.16) in both REC and RPC, respectively. Presented values correspond to the initial time (t=30 min) when the metabolic agents were added. To evaluate the consistency and reproducibility of the results, a total of 18 wells of each cell type were imaged, with n=6 for each of the treated groups. The slopes of the intensity profiles were calculated at the time of the administration of the agent for six FOV per group for the treated cells. The graphs in Fig. 2 show the average profile of the PCP, ROT, and AA experiments.

The slopes of the intensity right after the addition of mitochondrial metabolic modulators (t=30 min) were compared statistically in Fig. 3, demonstrating significant differences between REC and RPC. These slopes correlated with the intracellular ROS initiation rate

[6]. The red and blue bars in Fig. 3 represent initial ROS production rate in REC and RPC, respectively. These bars show greater rates of ROS production in REC by PCP, ROT, and AA, respectively, by a factor of 8.93 ± 1.18, 3.57 ± 0.27, and 5.64 ± 0.25 compared with RPC. Red and blue profiles in the top panel of Fig. 2 along with red and blue bars in Fig. 3 demonstrate the fastest and greatest increase in the rate of ROS production (8.93 ± 1.18) in uncoupled REC when compared with uncoupled RPC.

Intensity profiles in Fig. 4 compared ROS production and, hence, the metabolic resistivity of uncoupled REC with RPC under different glucose conditions including NG, OS, and HG. While blue profiles in the left panel (NG exposure) and green profiles in the right panel (OS condition) showed significantly smaller ROS production level and rate in uncoupled RPC compared with uncoupled REC, red profiles in bottom panel did not show any significant changes over time between the two cell types under HG condition.

The ROS initiation rates right after the addition of PCP (t = 30 min) in REC and RPC exposed to the different glucose conditions were compared statistically in Fig. 5. Bar graphs in Fig. 5 demonstrate significant changes in ROS initiation rate of REC group (red bars) compared with RPC group (blue bars) in response to different glucose conditions. The ROS initiation rates are summarized in table 1. The first row of this table (columns 1–3) corresponds to the stable response of the uncoupled REC to different glucose levels exposure without any significant changes between NG and HG groups. However, the second row of Table 1 shows the ROS initiation rates in uncoupled RPC with significant changes when incubated under different glucose conditions. The third row of table 1 is the p-values showing that ROS initiation rate in uncoupled RPC was significantly smaller than that of uncoupled REC under NG and OS conditions, but not under HG condition. Since OS was used to account for changes in osmolality of HG and to separate the effects of glucose from osmolality, OS-NG addresses the changes in ROS initiation rate due to osmolality. Therefore, the values of fifth column allow for quantifying the effect of only high glucose condition on the ROS initiation rate in REC and RPC. Comparing second and fifth columns, ROS initiation rates in uncoupled REC appeared with no significant changes, while uncoupled RPC showed a significant increase of 7.33 ± 0.16 times under high glucose condition (p-value= 1.26e-4).

4. Discussion

We demonstrated that fluorescence time-lapse microscopy using nano-molar Mito-SOX can be used as a tool for real-time monitoring of the mitochondrial ROS production in live cells. We believe this approach could have far-reaching implications for the assessment of ROS in physiology and pathophysiology. Utilizing this method, we investigated the metabolic resistivity of two types of retinal vascular cells, EC and PC. The dynamics of ROS production was determined over time before, during, and after cells were incubated with mitochondrial stressors. Moreover, to gain detailed insight into preferential bioenergetic sources impacted in REC and RPC, ROS generation rate was also studied under different glucose conditions including HG. A major finding of this study regarding the different metabolic activity of REC and RPC is that under normal glucose condition REC and RPC exhibited different sensitivity to mitochondrial stressors. Under HG condition, only the

metabolic resistivity of RPC was affected by the increase in glucose levels and showed an increase in ROS production rate. These results may provide a justification for the sensitivity of RPC to HG condition and/or diabetes [4].

Fig. 1(c) shows that the metabolic properties of REC and RPC are different even at normal glucose level. These results were further confirmed by stressing the mitochondria (Fig. 2 and 3) and observing that REC generate mitochondrial ROS with a greater rate compared with RPC in normal glucose. However, under high glucose (Fig. 1(d)) RPC generated more mitochondrial ROS while REC did not exceed the levels reached in normal glucose. These results suggest that high glucose has a minimal effect on the metabolic activity of REC and their mitochondrial ROS production.

The enhanced expression and activity of endothelial nitric oxide synthase (eNOS) may explain the inhibitive effect on mitochondrial ROS production in REC under HG. eNOS, which is expressed in EC [12] is responsible for most of the vascular nitric oxide (NO) production. NO mediates vasodilation by acting on perivascular supporting cells and also can act as a scavenger of superoxide anions maintaining a cellular balance of redox signaling in the endothelium in NG levels [13]. Huang et al. reported an enhanced expression of eNOS in retinal EC under HG [14]. The enhanced eNOS activity, and hence increased bioavailability of NO [15, 16] is consistent with the decreased generation rate of superoxide in retinal EC under HG. Moreover, the increased production of eNOS is shown to prevent apoptosis of EC under HG [17]. This may justify the decreased rate of apoptosis in REC compared to the RPC due to diabetes. However, the potential differences in glucose uptake in these cells cannot be ruled out.

The results in Fig. 2 and Fig. 3 show an increase in ROS production rate in both cell types, which is consistent with the notion that complexes I and III are the major sites of superoxide production in the presence of ROT [18–20] and AA [21–28]. Inhibiting complexes I and III with ROT [19] and AA [29, 30], fully reduces the chain upstream and blocks the electron transfer through these ETC complex sites [19, 31]. Impeding electron transfer leads to an electron buildup increasing the chance of the electron leak at these ETC complex sites and enhances superoxide formation [32, 33]. As a result, inhibiting complex I and III makes these complexes as major sites for electron leak and ROS production [18–22, 24–28, 34].

We found that mitochondrial uncoupling by PCP increased ROS production in both REC and RPC. PCP binds to mitochondrial proteins and inhibits mitochondrial ATPase activity. Thus, both the formation of ATP and the release of energy to the cell from the breakdown of ATP to ADP are prevented. Electron transport is not inhibited by PCP, although reactions dependent on available high-energy bonds, such as oxidative and glycolytic phosphorylation, are affected. Although glycolysis is the main source of ATP in cultured REC, the higher level of oxidative stress in uncoupled REC indicates that glycolysis and oxidative phosphorylation are linked for ATP production. Cultured REC are highly dependent on ATP for their activity. Since PCP inhibits mitochondrial ATPase activity, REC activate a mechanism to compensate for ATP and increase the ETC activity in the uncoupled chain [35]. This mechanism expedites the electron transfer through the chain leading to generation of more ROS. This does not appear to be the case for RPC. Lack of proton gradient for

phosphorylation and polarized membrane potential activates a mechanism to compensate for the uncoupling effect of PCP, by increasing proton pumping and respiration, to reestablish the proton gradient. Ironically, the increase in the activity of the complex I and II in the uncoupled chain [6, 36], increases electron transfer along the electron transport chain and as a result, increases electron leak to oxygen leading to superoxide production [29, 37–40].

Although RPC and REC are differentially affected by metabolic stress conditions, most likely because of their preferential bioenergetic sources, both cell types showed a higher rate of ROS production under stress. However, RPC were more resistive to mitochondrial stress under normal glucose condition when compared with REC. Right after incubation with mitochondrial stressor, REC showed a significantly greater increase in the rate of ROS production when compared with RPC. These results suggest that both inhibited REC and RPC metabolic activities, at least under normal glucose condition, may depend on the integrity of mitochondrial respiration. However, the reason for enhanced ROS generation in REC is not clear and requires further delineation of the bioenergetic pathways utilized by these cells. These may be linked to the oxygen and glucose levels. The use of different glucose and/or oxygen levels provides additional insight into the preferential bioenergetic pathway(s) utilized by these cells. However, the preferential utilization of glycolysis by REC as the major bioenergetic source suggests that REC may also depend on some intermediate metabolite(s), including those generated by isocitrate dehydrogenase 1, during respiration in order to maintain the cellular reductive state. Thus, attenuation of respiration could significantly reduce the level of such metabolite(s) and result in increased accumulation of ROS in REC.

We investigated the use of different glucose conditions in the current study, while the study of the effect of different oxygen conditions is subject of future investigation. Our results revealed a higher sensitivity of the RPC compared to REC under HG conditions. While under normal glucose condition the metabolic resistivity of RPC was greater than REC, but significantly decreased under HG condition triggering the pre-apoptosis process of the RPC. ROS over-production in this stage leads to a higher level of oxidative stress [41], which is known as an underlying mechanism causing the apoptosis of vascular cells associated with diabetic retinopathy. However, it remains unclear how HG condition leads to REC apoptosis. We have observed that incubation of REC under high glucose does not affect their rate of apoptosis [3]. Other studies suggest an indirect role for HG mediated REC death in retinal vasculature [42]. Thus, deterioration of vascular structure due to RPC loss may contribute to demise and dysfunction of REC in the retinal vasculature.

The disparity seen between RPC and REC may be also explained by the fact that mitochondrial oxygen consumption is compromised in RPC exposed to HG. Therefore, the extracellular acidification levels may be an influential factor in RPC. Trudeau et al. reported an increase in extracellular acidification levels in REC, possibly to compensate for HG-induced decreased mitochondrial oxygen consumption [43]. This compensation helps EC to maintain the rate of ROS generation with HG exposure without a significant increase compared to NG condition. Interestingly, the inability of the RPC to compensate for the HG-induced decrease in mitochondrial oxygen consumption, due to the significant decrease in extracellular acidification [43], indicates an increased susceptibility of the RPC to HG.

Moreover, the differential transport of glucose between the two cell types may also illustrate their different metabolic resistivity under HG condition. Previous reports have shown that HG downregulates Glut1 activity in PC, but not in EC [44]. Thus, different extracellular acidification levels and possibly glycolytic levels may indirectly lead to differential alternation of ROS production rate and metabolic resistivity in RPC and REC in response to HG exposure. Further research is required to indicate the mechanisms for the observed difference between the two cell types.

The findings of this study indicate that REC and RPC exhibit different responses to various mitochondrial and metabolic stress signals. Under normal glucose condition RPC only slightly responded to mitochondrial stress and generated significantly less ROS when compared with REC. Thus, RPC may utilize a different bioenergetic source for ATP production under normal glucose condition. In contrast, REC under NG condition may utilize mitochondrial respiration as a major bioenergetic source and generate more ROS, especially under mitochondrial stress. Under high glucose condition REC still remained sensitive to the effects of mitochondrial stressor without any additional effect from high glucose condition. This result confirms that HG minimally affects ROS levels in REC compared with NG. This is consistent with utilization of glycolysis as a primary bioenergetic source for ATP production and glucose metabolism in EC. In contrast, RPC under HG condition become more dependent on mitochondrial respiration as their bioenergetic source for glucose metabolism and generate more ROS. The exact identity of the bioenergetic sources utilized by these cells, especially under HG condition, awaits further confirmation.

Acknowledgements

UWM RGI 101×290; an unrestricted award from Research to Prevent Blindness to the Department of Ophthalmology; Retina Research Foundation; Environmental Protection Agency (EPA) 83573701; and National Institute of Health (NIH) P30 EY016665, P30 CA014520, EY022883, and EY026078. NS is a recipient of RPB Stein Innovation Award.

References

[1]. Cacicedo JM, Benjachareowong S, Chou E, Ruderman NB, and Ido Y, “Palmitate-induced apoptosis in cultured bovine retinal pericytes - Roles of NAD(P)H oxidase, oxidant stress, and ceramide,” (in English), Diabetes, vol. 54, no. 6, pp. 1838–1845, 6 2005. [PubMed: 15919807]

[2]. Kowluru RA, “Diabetic retinopathy: Mitochondrial dysfunction and retinal capillary cell death,” (in English), Antioxidants & Redox Signaling, vol. 7, no. 11–12, pp. 1581–1587, Nov-Dec 2005. [PubMed: 16356121]

[3]. Huang Q and Sheibani N, “High glucose promotes retinal endothelial cell migration through activation of Src, PI3K/Akt1/eNOS, and ERKs,” Am J Physiol Cell Physiol, vol. 295, no. 6, pp. C1647–57, 12 2008. [PubMed: 18945941]

[4]. Shin ES et al., “STAT1-mediated Bim expression promotes the apoptosis of retinal pericytes under high glucose conditions,” (in eng), Cell Death Dis, vol. 5, p. e986, 2014. [PubMed: 24407239]

[5]. Ghanian Z, “Quantitative Optical Studies of Oxidative Stress in Rodent Models of Eye and Lung Injuries,” PhD, University of Wisconsin Milwaukee, 2016.

[6]. Ghanian Z, Konduri GG, Audi SH, Camara AKS, and Ranji M, “Quantitative optical measurement of mitochondrial superoxide dynamics in pulmonary artery endothelial cells,” (in English), Journal of Innovative Optical Health Sciences, vol. 11, no. 1, 1 2018.

[7]. Grutzmacher C et al., “Opposing effects of bim and bcl-2 on lung endothelial cell migration,” (in eng), Am J Physiol Lung Cell Mol Physiol, vol. 299, no. 5, pp. L607–20, 11 2010. [PubMed: 20656893]

[8]. Su X, Sorenson CM, and Sheibani N, “Isolation and characterization of murine retinal endothelial cells,” Mol Vis, vol. 9, pp. 171–8, 5 1 2003. [PubMed: 12740568]

[9]. Scheef EA, Sorenson CM, and Sheibani N, “Attenuation of proliferation and migration of retinal pericytes in the absence of thrombospondin-1,” (in English), American Journal of Physiology-Cell Physiology, vol. 296, no. 4, pp. C724–C734, 4 2009. [PubMed: 19193867]

[10]. Ghanian Z, Konduri GG, Audi SH, Camara AKS, and Ranji M, “Quantitative optical measurement of mitochondrial superoxide dynamics in pulmonary artery endothelial cells,” Journal of Innovative Optical Health Sciences, vol. 0, no. 0, p. 1750018.

[11]. Ghanian Z et al., “Quantitative Assessment of Retinopathy Using Multi-parameter Image Analysis,” J Med Signals Sens, vol. 6, no. 2, pp. 71–80, Apr-Jun 2016. [PubMed: 27186534]

[12]. Forstermann U and Sessa WC, “Nitric oxide synthases: regulation and function,” Eur Heart J, vol. 33, no. 7, pp. 829–37, 837a-837d, 4 2012. [PubMed: 21890489]

[13]. Sessa WC, “Regulation of endothelial derived nitric oxide in health and disease,” Mem Inst Oswaldo Cruz, vol. 100 Suppl 1, pp. 15–8, 3 2005. [PubMed: 15962093]

[14]. Huang Q and Sheibani N, “High glucose promotes retinal endothelial cell migration through activation of Src, PI3K/Akt1/eNOS, and ERKs,” (in English), American Journal of Physiology-Cell Physiology, vol. 295, no. 6, pp. C1647–C1657, 12 2008. [PubMed: 18945941]

[15]. El-Remessy AB, Abou-Mohamed G, Caldwell RW, and Caldwell RB, “High glucose-induced tyrosine nitration in endothelial cells: role of eNOS uncoupling and aldose reductase activation,” Invest Ophthalmol Vis Sci, vol. 44, no. 7, pp. 3135–43, 7 2003. [PubMed: 12824263]

[16]. Fleming I and Busse R, “Molecular mechanisms involved in the regulation of the endothelial nitric oxide synthase,” Am J Physiol Regul Integr Comp Physiol, vol. 284, no. 1, pp. R1–12, 1 2003. [PubMed: 12482742]

[17]. Ho FM, Liu SH, Liau CS, Huang PJ, Shiah SG, and Lin-Shiau SY, “Nitric oxide prevents apoptosis of human endothelial cells from high glucose exposure during early stage,” J Cell Biochem, vol. 75, no. 2, pp. 258–63, 11 1 1999. [PubMed: 10502298]

[18]. Brueckl C et al., “Hyperoxia-induced Reactive Oxygen Species Formation in Pulmonary Capillary Endothelial Cells in situ,” Am J Respir Cell Mol Biol, 12 15 2005.

[19]. Turrens JF, “Mitochondrial formation of reactive oxygen species,” J Physiol, vol. 552, no. Pt 2, pp. 335–44, 10 15 2003. [PubMed: 14561818]

[20]. Kallet RH and Matthay MA, “Hyperoxic acute lung injury,” Respir Care, vol. 58, no. 1, pp. 123–41, 1 2013. [PubMed: 23271823]

[21]. Cadenas E, Boveris A, Ragan CI, and Stoppani AO, “Production of superoxide radicals and hydrogen peroxide by NADH-ubiquinone reductase and ubiquinolcytochrome c reductase from beef-heart mitochondria,” (in eng), Arch Biochem Biophys, vol. 180, no. 2, pp. 248–57, 4 30 1977. [PubMed: 195520]

[22]. Turrens JF, Alexandre A, and Lehninger AL, “Ubisemiquinone is the electron donor for superoxide formation by complex III of heart mitochondria,” (in eng), Arch Biochem Biophys, vol. 237, no. 2, pp. 408–14, 3 1985. [PubMed: 2983613]

[23]. Volpert OV et al., “Id1 regulates angiogenesis through transcriptional repression of thrombospondin-1,” Cancer Cell, vol. 2, no. 6, pp. 473–83, 12 2002. [PubMed: 12498716]

[24]. Zhang L, Yu LD, and Yu CA, “Generation of superoxide anion by succinatecytochrome c reductase from bovine heart mitochondria,” (in English), Journal of Biological Chemistry, vol. 273, no. 51, pp. 33972–33976, 12 18 1998. [PubMed: 9852050]

[25]. Rich PR and Bonner WD, “The sites of superoxide anion generation in higher plant mitochondria,” (in eng), Arch Biochem Biophys, vol. 188, no. 1, pp. 206–13, 5 1978. [PubMed: 209742]

[26]. Grigolava IV, Ksenzenko M, Konstantinob AA, Tikhonov AN, and Kerimov TM, “[Tiron as a spin-trap for superoxide radicals produced by the respiratory chain of submitochondrial particles],” (in rus), Biokhimiia, vol. 45, no. 1, pp. 75–82, 1 1980. [PubMed: 6260236] Tairon

kak spinovaia lovushka dlia superoksidnykh radikalov, obrazuemykh dykhatel'noi tsep'iu sybmitokhondrial'nykh chastits.

[27]. Mukhopadhyay P, Rajesh M, Hasko G, Hawkins BJ, Madesh M, and Pacher P, "Simultaneous detection of apoptosis and mitochondrial superoxide production in live cells by flow cytometry and confocal microscopy," (in English), Nature Protocols, vol. 2, no. 9, pp. 2295–2301, 2007. [PubMed: 17853886]

[28]. Robinson KM et al., "Selective fluorescent imaging of superoxide in vivo using ethidium-based probes," (in English), Proceedings of the National Academy of Sciences of the United States of America, vol. 103, no. 41, pp. 15038–15043, 10 10 2006. [PubMed: 17015830]

[29]. Cadenas E and Boveris A, "Enhancement of hydrogen peroxide formation by protophores and ionophores in antimycin-supplemented mitochondria," Biochem J, vol. 188, no. 1, pp. 31–7, 4 15 1980. [PubMed: 7406888]

[30]. Ksenzenko M, Konstantinov AA, Khomutov GB, Tikhonov AN, and Ruuge EK, "Effect of electron transfer inhibitors on superoxide generation in the cytochrome bc1 site of the mitochondrial respiratory chain," FEBS Lett, vol. 155, no. 1, pp. 19–24, 5 2 1983. [PubMed: 6301880]

[31]. St-Pierre J, Buckingham JA, Roebuck SJ, and Brand MD, "Topology of superoxide production from different sites in the mitochondrial electron transport chain," J Biol Chem, vol. 277, no. 47, pp. 44784–90, 11 22 2002. [PubMed: 12237311]

[32]. Stowe DF and Camara AK, "Mitochondrial reactive oxygen species production in excitable cells: modulators of mitochondrial and cell function," Antioxid Redox Signal, vol. 11, no. 6, pp. 1373–414, 6 2009. [PubMed: 19187004]

[33]. Lee S et al., "Mitochondrial H2O2 generated from electron transport chain complex I stimulates muscle differentiation," Cell Res, vol. 21, no. 5, pp. 817–34, 5 2011. [PubMed: 21445095]

[34]. Liu Y, Fiskum G, and Schubert D, "Generation of reactive oxygen species by the mitochondrial electron transport chain," (in eng), Journal of Neurochemistry, vol. 80, no. 5, pp. 780–7, 3 2002. [PubMed: 11948241]

[35]. Kalbacova M, Vrbacky M, Drahota Z, and Melkova Z, "Comparison of the effect of mitochondrial inhibitors on mitochondrial membrane potential in two different cell lines using flow cytometry and spectrofluorometry," (in eng), Cytometry A, vol. 52, no. 2, pp. 110–6, 4 2003. [PubMed: 12655654]

[36]. Sepehr R, Audi SH, Staniszewski KS, Haworth ST, Jacobs ER, and Ranji M, "Novel Flurometric Tool to Assess Mitochondrial Redox State of Isolated Perfused Rat Lungs after Exposure to Hyperoxia," IEEE J Transl Eng Health Med, vol. 1, 10 16 2013.

[37]. Dong YL, Zhou PJ, Jiang SY, Pan XW, and Zhao XH, "Induction of oxidative stress and apoptosis by pentachlorophenol in primary cultures of Carassius carassius hepatocytes," (in English), Comparative Biochemistry and Physiology C-Toxicology & Pharmacology, vol. 150, no. 2, pp. 179–185, 8 2009.

[38]. Aon MA, Cortassa S, and O'Rourke B, "Redox-optimized ROS balance: A unifying hypothesis," (in English), Biochimica Et Biophysica Acta-Bioenergetics, vol. 1797, no. 6–7, pp. 865–877, Jun-Jul 2010.

[39]. Farrahi Moghaddam J, Nakhaee N, Sheibani V, Garrusi B, and Amirkafi A, "Reliability and validity of the Persian version of the Pittsburgh Sleep Quality Index (PSQI-P)," (in eng), Sleep Breath, vol. 16, no. 1, pp. 79–82, 3 2012. [PubMed: 21614577]

[40]. Feissner RF, Skalska J, Gaum WE, and Sheu SS, "Crosstalk signaling between mitochondrial Ca2+ and ROS," (in English), Frontiers in Bioscience-Landmark, vol. 14, pp. 1197–1218, 1 1 2009.

[41]. Giacco F and Brownlee M, "Oxidative stress and diabetic complications," Circ Res, vol. 107, no. 9, pp. 1058–70, 10 29 2010. [PubMed: 21030723]

[42]. Busik JV, Mohr S, and Grant MB, "Hyperglycemia-induced reactive oxygen species toxicity to endothelial cells is dependent on paracrine mediators," Diabetes, vol. 57, no. 7, pp. 1952–65, 7 2008. [PubMed: 18420487]

[43]. Trudeau K, Molina AJA, and Roy S, “High Glucose Induces Mitochondrial Morphology and Metabolic Changes in Retinal Pericytes,” (in English), Investigative Ophthalmology & Visual Science, vol. 52, no. 12, pp. 8657–8664, 11 2011. [PubMed: 21979999]

[44]. Mandarino LJ, Finlayson J, and Hassell JR, “High glucose downregulates glucose transport activity in retinal capillary pericytes but not endothelial cells,” (in eng), Invest Ophthalmol Vis Sci, vol. 35, no. 3, pp. 964–72, 3 1994. [PubMed: 8125759]

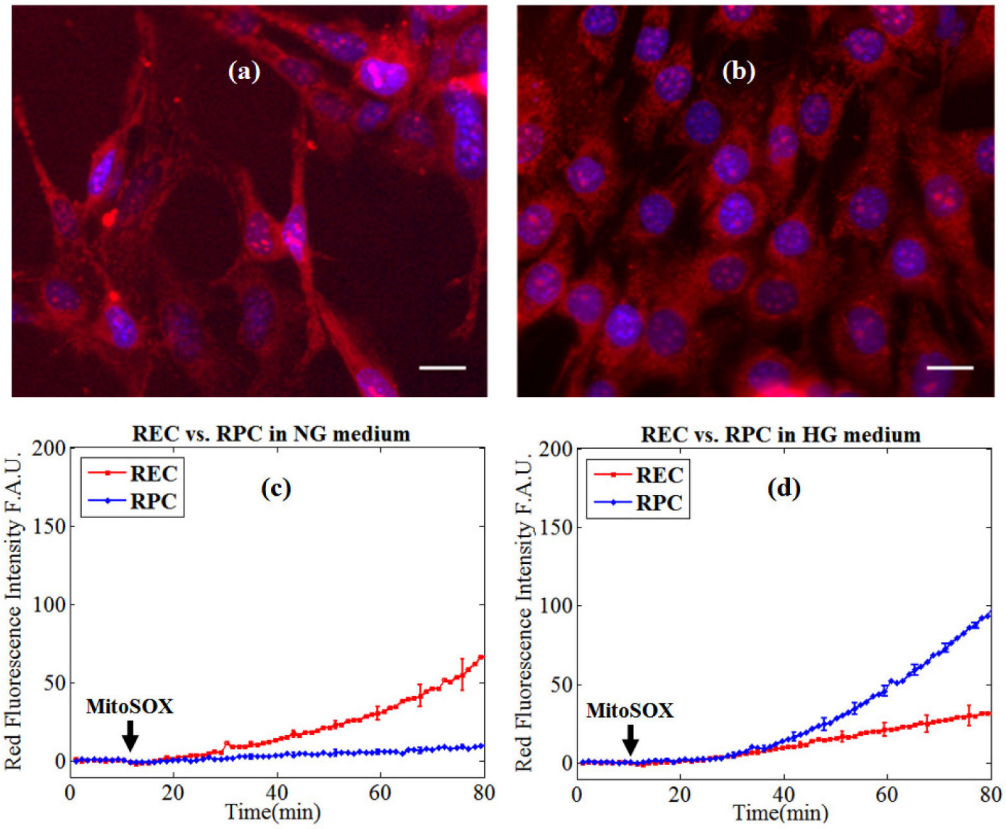

Fig. 1.

Top panels: Overlay of the blue (Hoechst) and MitoSOX red fluorescence signals. Note that the scale bar represents 32 μm (~100 pixels); a) retinal endothelial cells (REC); b) retinal pericytes (RPC). Bottom panels: Comparing resistivity of REC and RPC under normal glucose (NG) and high glucose (HG) conditions; c) The fluorescence intensity profiles of REC and RPC in NG; d) Fluorescence intensity profiles of REC and RPC in HG.

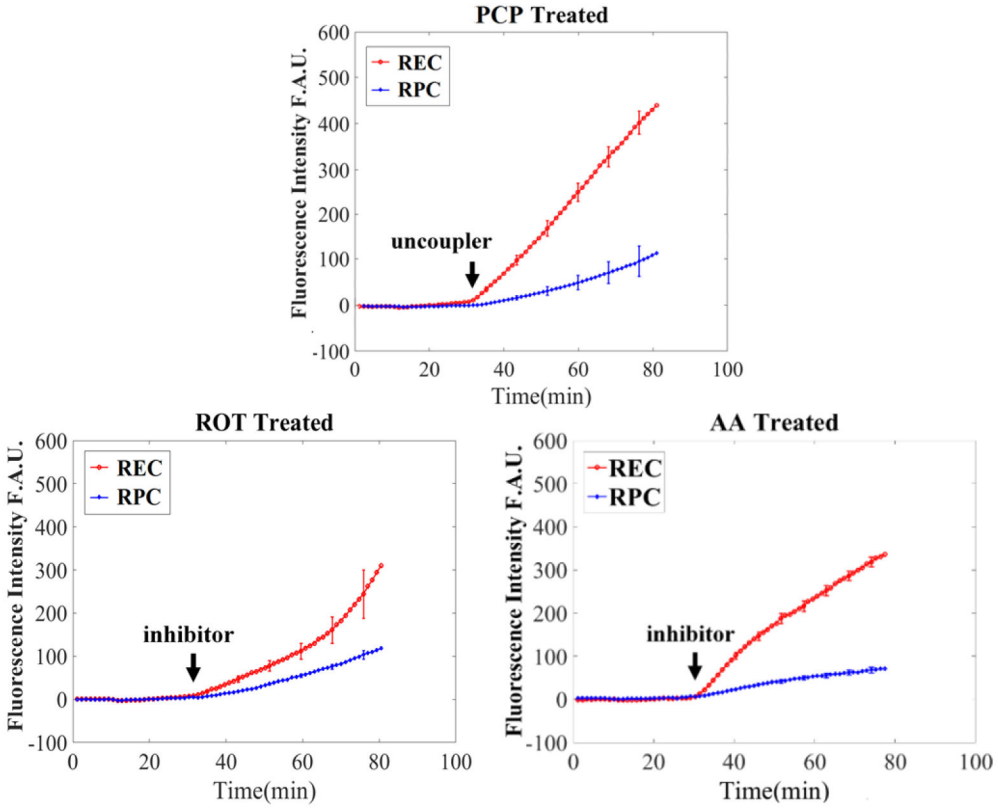

Fig. 2.

Comparing resistivity of REC and RPC under metabolic stress and normal glucose condition (NG); Top panel: Fluorescence intensity (ROS production) profiles of REC and RPC in uncoupled ETC; Bottom panels: Fluorescence intensity (ROS production) profiles of REC and RPC in inhibited ETCs.

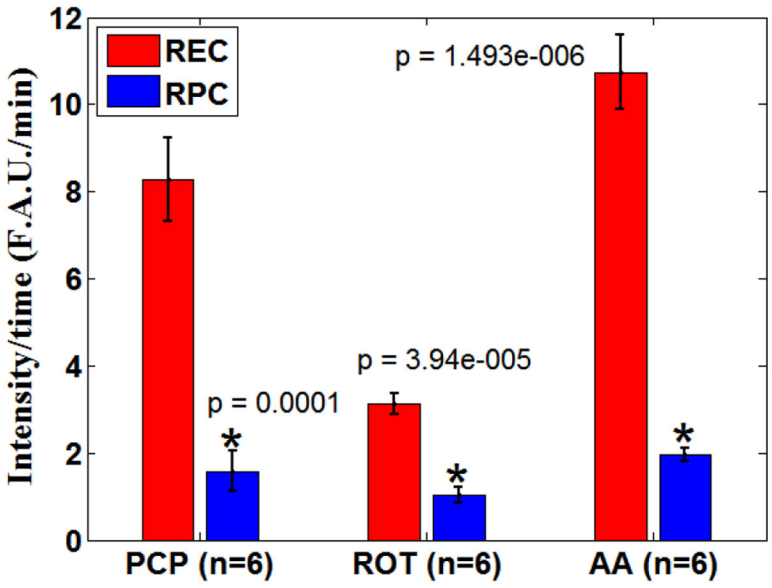

Fig. 3.

Summary bar graphs show the statistical analysis (mean ± SE) of *ROS initiation rate (at 30 min)* in live retina cells in normal glucose condition induced by metabolic uncoupler (PCP), and inhibitors (ROT, AA).

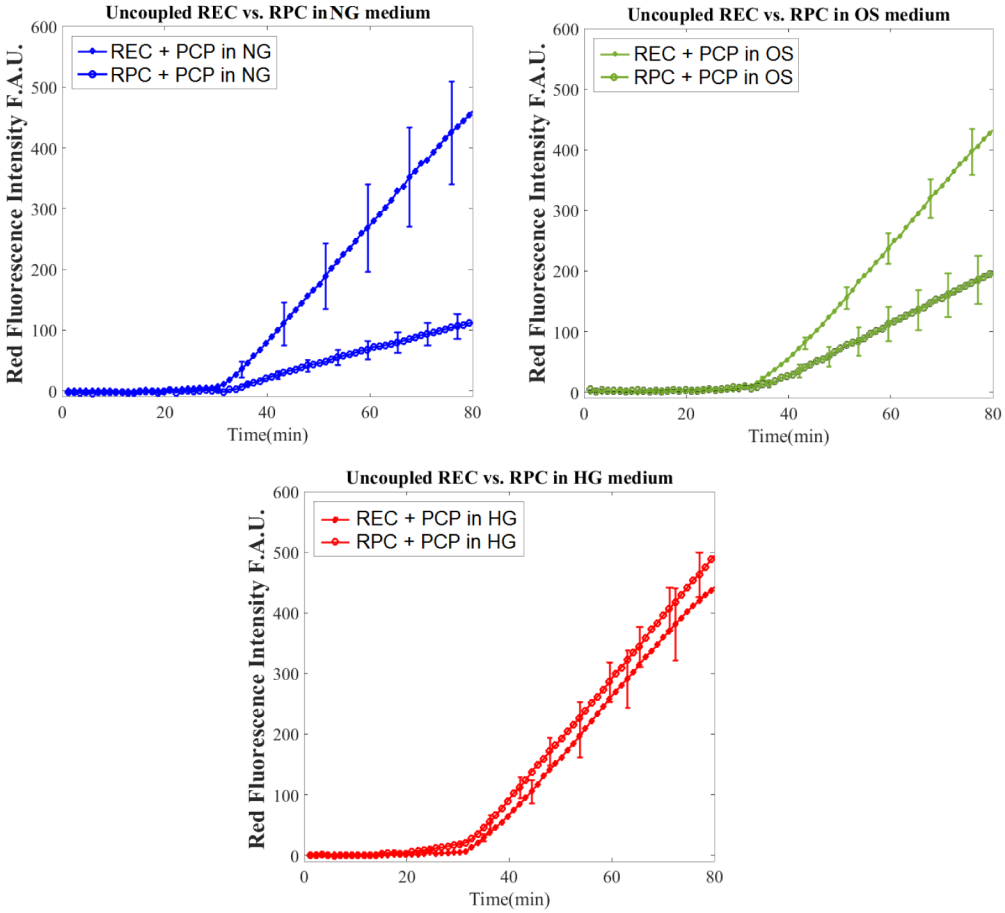

Fig. 4.

Fluorescence intensity profiles comparing the metabolic resistivity of *uncoupled* REC and RPC under different glucose exposures including NG, OS, and HG (n=6/group).

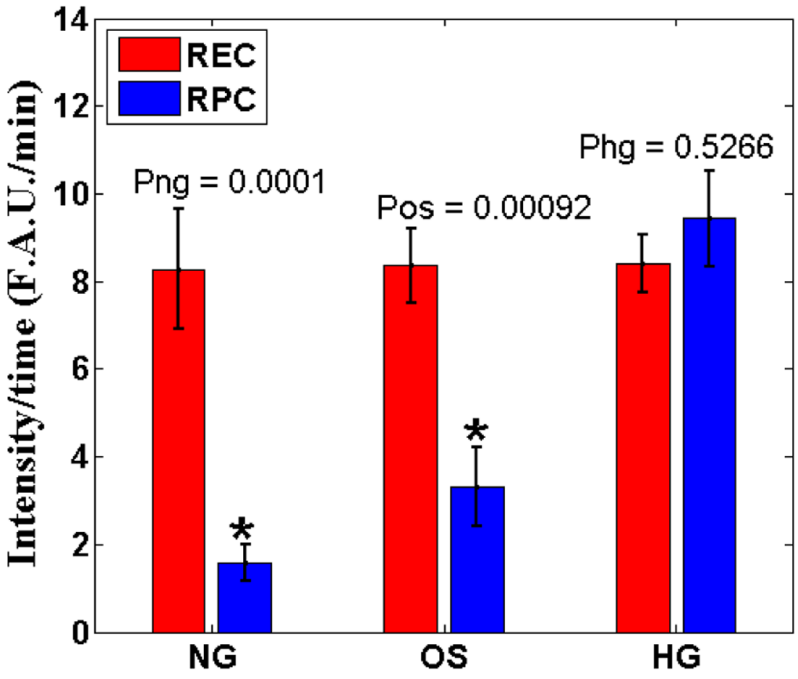

Fig. 5.

Bar graphs demonstrate the statistical analysis (mean ± SE) of *ROS initiation rate (at 30 min)* induced by PCP in live retina cells in NG, OS, and HG exposures (n=6/group).

Table 1.

ROS initiation rate comparison in uncoupled REC versus uncoupled RPC exposed to different glucose level

	NG	OS	HG	HG-(OS-NG)
REC	8.27 ± 0.97	8.35 ± 0.85	8.41 ± 0.66	8.68 ± 0.24
RPC	1.58 ± 0.47	3.30 ± 0.91	9.43 ± 1.08	7.72 ± 0.20
P-value	0.0001	0.0009	0.5266	0.0025